PO-0866: Visibility, image artifacts and proton dose perturbation of fiducial markers

Hamming, V.C.; Brouwer, C.L.; Goethem, M.J. Van; Jolck, R.I.; Leijsen, C. Van; Bergh, A.C.M. Van den

DOI:
10.1016/S0167-8140(17)31303-8

fiducials were used. Optimal positioning of the fiducials did not improve the accuracy of the treatment when compared to the accuracy achieved with typical clinical fiducial positions or with three fiducials. Usage of only two fiducials in the target tracking resulted clinically unacceptable accuracy.

PO-0865 Commissioning and clinical implementation of intra-fractional 4D-CBCT imaging for lung SBRT

R. Sims[1]
[1]*ARO - Auckland Radiation Oncology, Radiotherapy Physics, Auckland, New Zealand*

Purpose or Objective

Geometric verification of the tumour for free-breathing lung SBRT patients is challenging due to limitations of CBCT imaging at the treatment unit. This can be overcome by using novel acquisition and reconstruction tools to produce a 4D-CBCT dataset that can be acquired both before (inter-fraction) and during (intra-fraction) beam delivery. The commissioning and clinical experience of such a system for lung SBRT will be presented.

Material and Methods

An anthropomorphic phantom was used to investigate system efficacy for identifying changes in reconstructed motion with different acquisition settings for a variety of clinical situations. The sensitivity of the system to detect changes to programmed motion was investigated and compared to baseline 4DCT imaging with changes to image quality and kV absorbed dose being quantified using additional phantoms. The use of the system during MV treatment for VMAT deliveries was investigated and compared to baseline 4D-CBCT imaging with overall system performance being assessed in terms of image quality and image registration accuracy at the treatment console.

Results

For inter-fraction imaging, the system successfully identifies changes in amplitude motion to within ±2mm and is sensitive to image distortion/artefacts with different/irregular respiratory cycles and number of image projections. The absorbed dose for standard scan settings is 23.0 ± 1.6mGy with registration accuracy of ±0.4mm and ±0.3degrees. When used intra-fraction there is a reduction in image quality owing to the dependence on VMAT delivery and MV scatter. This can be seen in Figure 1 as a function of VMAT arc length, with the quicker arcs resulting in poorer image quality (for a given BPM of the phantom). Measuring this in terms of contrast-to-noise ratio (between the tumour and surrounding lung tissue) demonstrates that as the arc length and breathing rate increases, the contrast-to-noise ratio approaches that of the inter-fraction 4D-CBCT (see Figure 2). The automatic 4D matching algorithm was found to be influenced by image noise, causing a reduction in the measured amplitude of tumour motion, however despite this the accuracy of automatic registration was excellent varying by ±0.9mm (2SD) for compared to inter-fraction imaging baselines.

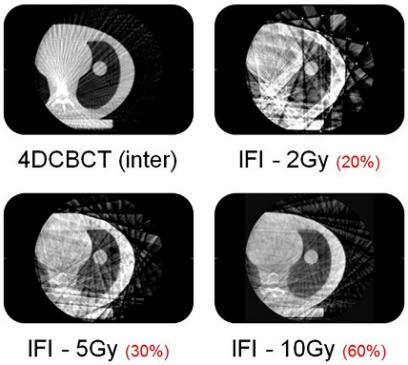

Figure 1 – Illustration of the different image artefacts that are apparent when using 4DCBCT in inter- and intra-fractional imaging (IFI) modes. The IFI results for 2Gy, 5Gy and 10Gy arcs are shown; with the red text demonstrating the percentage of data that has been used in the reconstruction (i.e. 2Gy arc contains only 20% of image frames compared to inter-fractional imaging).

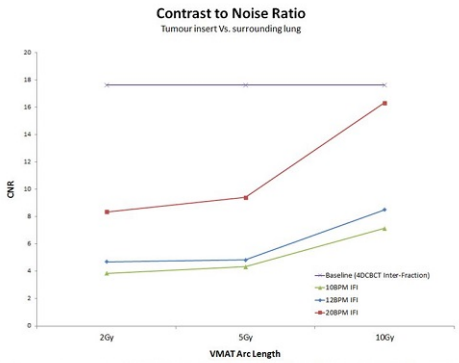

Figure 2 – Contrast to noise results for the tumour insert and surrounding lung for the same phantom as shown in Figure 1. The baseline is inter-fractional 4DCBCT imaging with the increasing CNR results apparent as the BPM of the phantom increases, and the arc length increases, as the sampling (degree/projections) increase. Note that although the number of projections for the 10Gy 208PM data point exceeds the baseline, the CNR is lower. This is related to limitations of the MV scatter correction algorithm.

Conclusion

Intra-fractional 4D-CBCT imaging has been implemented successfully and is now mandated for all lung SBRT patients at our clinic. The system has also been implemented for 3D spinal SBRT imaging although limitations of the MV scatter correction algorithm have resulted in our centre limiting the MU/Arc for VMAT delivery for these cases. Future studies will investigate different acquisition methods for existing conventionally-fractionated treatments to improve the workflow and improve image quality.

Poster: Physics track: Inter-fraction motion management (excl. adaptive radiotherapy)

PO-0866 Visibility, image artifacts and proton dose perturbation of fiducial markers

V.C. Hamming[1], C.L. Brouwer[1], M.J. Van Goethem[1], R.I. Jolck[2], C. Van Leijsen[1], A.C.M. Van den Bergh[1]
[1]*UMCG University Medical Center Groningen, Radiation Oncology, Groningen, The Netherlands*
[2]*NANOVI radiotherapy, DTU scion, Lyngby, Denmark*

Purpose or Objective

Fiducial markers (FMs) are necessary for an accurate photon and proton radiation treatment for prostate-cancer. However, conventional FMs may cause problems with dose calculations and perturbations in proton therapy. Therefore, specific proton-treatment FMs are available having smaller dimensions and different material compositions. The goal of this research was to survey the visibility, CT artifacts and proton dose perturbations of available FMs to choose the optimal FM for proton therapy.

Material and Methods

The FMs used in this research were: BioXmark (NANOVI, 300, 100, 50, 25 and 10µL (liquid)), BiomarC (Carbon Medical Technologies, Enhanced (1x5mm), Pro (0.9x5mm) and Standard (1x5mm)), Visicoil (IBA, 0.75x5mm, 0.5x5mm), GoldAnchor (Naslund Medical, 0.28x10mm (open and folded)) and the fiducial gold marker (1x5mm, 0.4x5mm). All these FMs were positioned in a gelatin phantom. The above mentioned FMs were rated for the marker visibility on CT (with and without image metal artifact reduction (IMAR)), MRI, 3D-CBCT (low (±36.6mAs) and high (±234.9mAs) dose) and MV imaging by means of the contrast to noise ratio (CNR). A CNR ≤ 1 was considered not visible whereas a CNR ≥ 5 was considered as visible. For the CT image the streak index (SI) was determined as well and was normalized to the fiducial gold marker (1x5mm). A normalized SI of 0 was considered to have no artifact, whereas a normalized SI of 1 was considered to have the largest artifact amongst the FM.

Proton perturbation film measurements in a solid water phantom (SWP) were done at four different depths (5.4, 5.6, 6.1, 7.1cm) for a selection of the FMs: fiducial gold marker 1x5mm, 0.4x5mm and the GoldAnchor 0.28x10mm folded. A circular (50mm diameter) proton beam of 190 MeV was used to irradiate a dose of 7Gy in the Bragg peak. The Bragg peak was calculated to be at a depth of 7.1cm within the SWP.

Needle sizes were also taken into account with regard to the necessity to temporarily stop anticoagulants.**Results**

All FMs were visible on CT (Figure 1). Most of the FMs were visible on MRI except for the GoldAnchor (open), BiomarC (standard) and the visicoils. On 3D-CBCT all FMs were visible. In MV imaging for photon radiation treatment the fiducial gold marker (1x5mm) and visicoil (0,75x5mm) were visible. The SI was maximal for the FM with gold and minimal for the BioXmark FM (Table 1).

The fiducial gold marker (1x5mm) had the maximal proton dose perturbation measured which resulted in 10% underdosage at a depth of 7.1cm. For the other selected FMs no dose perturbation could be detected.

BioXmark and GoldAnchor can be placed with the small 25G needle.

Figure 1: Overview of images from different imaging modalities. (A) CT images (3mm), from left to right: BiomarC standard, Visicoil 0.75x5mm, Visicoil 0.5x5mm, fiducial gold 1x5mm, fiducial gold 0.4x5mm, BioXmark 300uL, 100uL, 50uL, 25uL, 10uL, GoldAnchor 0.28x10mm open, GoldAnchor 0.28x10mm folded, BiomarC enhanced, BiomarC pro. (B) CT images (3mm + IMAR). (C) 3DCBCT head and neck protocol. (D) 3DCBCT thoracic protocol. (E) MRI images (standard medic prostate protocol). (F) MV images from the top view, 8MU and 4MU respectively. (G) MV images from the lateral view, 8MU and 4MU respectively.

		Contrast to Noise Ratio										Streak Artifact Index	Needle size	Fiducial Marker material
							MV					Normalized to goldmarker 1x5mm		
		CT		MRI	CBCT		Anterior-posterior view		Lateral view			CT		
		3mm	3mm (IMAR)	Prostate-protocol	Low dose	High dose	4MU	8MU	4MU	8MU		3mm	3mm (IMAR)		
BioXmark	300uL	272,76	252,54	16,51	64,95	95,05	- *	-	-	-		0,85	0,78	(liquid) 25G**	Liquid iodine based
	100uL	73,92	132,16	14,98	11,76	15,18	-	-	-	-		0,84	0,79	(liquid) 25G	Liquid iodine based
	50uL	39,11	82,96	71,45	11,60	12,46	-	-	-	-		0,87	0,81	(liquid) 25G	Liquid iodine based
	25uL	8,47	20,11	4,20	11,24	8,08	-	-	-	-		0,65	0,64	(liquid) 25G	Liquid iodine based
	10uL	3,87	6,78	5,92	2,99	2,16	-	-	-	-		0,56	0,57	(liquid) 25G	Liquid iodine based
Gold Anchor	open (0.28x10mm)	2,32	3,19	0,77	7,01	2,85	-	-	-	-		0,80	0,81	25G	Gold
	folded (0.28x10mm)	3,40	7,64	13,27	7,40	5,12	1,36	0,83	-	-		0,81	0,80	25G	Gold
BiomarC	enhanced (1x5mm)	3,77	10,00	14,65	5,95	4,04	-	-	-	-		0,74	0,77	19G	Pyrolytic carbon coated Zirconium oxide
	pro (0.9x5mm)	6,45	233,69	14,01	6,77	5,61	-	-	-	-		0,95	0,96	18G	Pyrolytic carbon coated Zirconium oxide
	standard (1x5mm)	4,57	4,09	1,80	5,48	4,02	-	1,34	-	-		0,63	0,65	18G	Pyrolytic carbon coated Zirconium oxide
Visicoil	0,75x5mm	7,44	10,11	2,20	2,10	2,69	4,29	4,91	4,80	5,90		0,99	0,98	<21G	Gold
	0,5x5mm	6,63	5,92	1,42	3,48	3,75	2,22	2,54	2,14	2,81		0,91	0,95	21G	Gold
GoldMarker	1x5mm	248,15	240,02	5,13	23,48	19,17	4,35	5,01	5,09	7,99		1,00	1,00	18G	Gold
	0,4x5mm	39,61	42,49	11,91	3,07	5,91	1,86	2,09	-	1,43		0,92	0,93	>18G	Gold

Table 1: Overview of the different FMs regarding the contrast to noise ratio, streak artifact index, needle size and material composition. Red values are considered to have low visibility (≤2.5 CNR).
* - Not Visible
** 25G needles have an outer diameter of 0.51mm whereas a 18G needle has an outer diameter of 1.25mm

Conclusion

The FM BioXmark 25 µL resulted in high visibility, low streak artifacts and smallest needle size.

BioXmark is expected to have a smaller dose perturbation than was researched, because it has a lower atomic number and density than gold based FMs. In case larger volumes are needed a perturbation may become noticeable.

PO-0867 Magnitude and robustness of motion mitigation in stereotactic body radiation therapy of the liver

C. Heinz[1], S. Gerum[1], F. Kamp[1], M. Reiner[1], F. Roeder[1]
[1]*LMU Munich, Department of Radiation Oncology, Munich, Germany*

Purpose or Objective

SBRT has been established as an effective treatment method of lesions located in the liver. However, respiratory induced motion has to be taken into account for tumor delineation and without proper motion mitigation techniques motion will result in undesirable increased treatment volumes. Abdominal compression has been described as an effective way to limit respiratory induced motion and thereby decrease treatment volumes. However, the whole workflow of motion estimation (4DCT), motion mitigation (abdominal compression), motion incorporation into planning (ITV delineation) and motion evaluation at each fraction (CBCT) depends strongly on the available equipment and is thereby specific to each department. Hence the achievable results in motion management are specific to a department and should be assessed. In this retrospective study the magnitude and robustness of abdominal compression was compared to a free breathing workflow using the specific equipment in our clinic.

Material and Methods

A total of 26 patients (abdominal compression n=11; free breathing n=15) that were treated with SBRT of the liver during 2011-2016 were analysed. Prior to the initial imaging fiducial markers were implanted next to each treatment target. Each patient received a 4DCT (Toshiba Medical Systems Corporation, Tokyo, Japan) from which a mean intensity projection CT (Mean CT) was generated (iPlan, Brainlab AG, Munich, Germany). Pre-treatment imaging included a conventional 3D-CBCT (Elekta AB, Stockholm, Sweden). Abdominal compression was realised using the BodyFIX system (Elekta AB, Stockholm, Sweden). Overall 74 fiducial markers (abdominal compression n=28; free breathing n=46) were analysed with regard to respiratory induced motion in the mean intensity projection CT as well as in all available 3D-CBCTs using an in-house developed software tool. The software provided a semi-automatic marker segmentation of the blurred markers and a motion estimation of the segmented markers using a principal component analysis. The estimated motion from the initial imaging was compared to the motion estimated from the pre-treatment imaging in all major axes and 3D distance in magnitude (mean value) and robustness (standard deviation).

Results

Under free breathing patient data showed a mean marker movement (3D) of 19.8 mm in the Mean CT and 18.7 mm in the CBCT. By using the abdominal compression tool the mean marker movement was reduced to 15.7 mm in the Mean CT and 13.2 mm in the CBCT. Also the standard deviation of the 3D marker movement was reduced from 3.6 mm to 1.7 mm in the Mean CT data and from 3.8 mm to 2.7 mm in the CBCT data (see figure 1).